Geophysical Research Letters

RESEARCH LETTER
10.1029/2024GL110994

Constrained Projections Indicate Less Delay in Onset of Summer Monsoon over the Bay of Bengal and South China Sea

Yifeng Cheng[1], Lu Wang[1,2], Xiaolong Chen[3], Tianjun Zhou[3,4], Andrew Turner[5,6], and Lijuan Wang[1]

[1]Key Laboratory of Meteorological Disaster, Ministry of Education (KLME)/Collaborative Innovation Center on Forecast and Evaluation of Meteorological Disasters (CIC-FEMD), Nanjing University of Information Science and Technology, Nanjing, China, [2]Laboratory for Regional Oceanography and Numerical Modeling, Qingdao Marine Science and Technology Center, Qingdao, China, [3]State Key Laboratory of Numerical Modeling for Atmospheric Sciences and Geophysical Fluid Dynamics, Institute of Atmospheric Physics, Chinese Academy of Sciences, Beijing, China, [4]College of Earth and Planetary Sciences, The University of Chinese Academy of Sciences, Beijing, China, [5]National Centre for Atmospheric Science, University of Reading, Reading, UK, [6]Department of Meteorology, University of Reading, Reading, UK

Key Points:

- An observational constraint is identified for projected changes in summer monsoon onset date over the Bay of Bengal and South China Sea
- Models with a warmer sea surface temperature bias over the tropical western Pacific tend to project a more delayed monsoon onset in the future
- The emergent constraint indicates that the delay of monsoon onset over the Bay of Bengal and South China Sea is overestimated

Supporting Information:

Supporting Information may be found in the online version of this article.

Correspondence to:

L. Wang,
luwang@nuist.edu.cn

Citation:

Cheng, Y., Wang, L., Chen, X., Zhou, T., Turner, A., & Wang, L. (2024). Constrained projections indicate less delay in onset of summer monsoon over the Bay of Bengal and South China Sea. *Geophysical Research Letters*, *51*, e2024GL110994. https://doi.org/10.1029/2024GL110994

Received 23 JUN 2024
Accepted 15 OCT 2024

Author Contributions:

Conceptualization: Lu Wang
Formal analysis: Yifeng Cheng, Lu Wang
Funding acquisition: Lu Wang
Investigation: Yifeng Cheng
Methodology: Yifeng Cheng, Xiaolong Chen
Supervision: Lu Wang
Writing – original draft: Yifeng Cheng, Lu Wang
Writing – review & editing: Lu Wang, Xiaolong Chen, Tianjun Zhou, Andrew Turner, Lijuan Wang

Abstract The summer monsoon onset over the Bay of Bengal and South China Sea signals the beginning of the Asian summer monsoon, critical for local fisheries, agriculture and livelihoods, so communities are concerned about its potential changes under global warming. Previous projections have suggested a delay, but the extent of this delay remains uncertain, undermining the reliability of the projections. Here, we show a significant correlation between the projected shift in Bay of Bengal/South China Sea monsoon onset and present-day sea surface temperature (SST) simulation over the western Pacific (WP). This emergent relationship arises from the spread of the precipitation response over the western-central Pacific to WP SST, as more precipitation induces stronger tropical upper-tropospheric warming, increasing westerly vertical shear near South Asia, and facilitating the onset delay. The rectified projections indicate that the delayed shift is almost halved compared to raw projections, and the intermodel uncertainty is reduced by 30%.

Plain Language Summary The summer monsoon onset over the Bay of Bengal and South China Sea is a crucial time for fishing, agriculture and livelihood, and is important for the further advance of the monsoon rains over tropical Asia. Previous studies have suggested that monsoon onset in these seas will be delayed in the future, but there is large uncertainty between models, undermining the reliability of the projection. This study finds that the projected shift in the onset is strongly related to a model's representation of sea surface temperatures over the western Pacific Ocean in the present day. Based on the relationship found in observations, we adjust or "constrain" the future projections of the monsoon onset. The delay to the monsoon onset using this adjustment is almost half of the original projection, and the uncertainty between models is also reduced. We suggest that a more accurate simulation of sea-surface temperatures in the present-day climate of the western Pacific Ocean is crucial for reliable future projections of the monsoon onset.

1. Introduction

The onset of the Asian summer monsoon begins in the Bay of Bengal (BoB) and South China Sea (SCS) basins, typically during early to mid-May (Wang & LinHo, 2002). Variations in monsoon onset timing over the BoB and SCS (B–S) can have significant impacts on the social and economic well-being of coastal residents in South and Southeast Asia (e.g., Bombardi et al., 2019). For example, if the B–S monsoon occurs earlier than usual, it can cause an earlier fishing moratorium period in the affected areas (Islam et al., 2021), increase the frequency of cyclones over these areas (Wang & Chen, 2018), and hasten the subsequent march of the monsoon rainbelt, which leads to the establishment of the monsoon over the land (Jiang et al., 2018). As anthropogenic warming has a great influence on monsoon systems (Arias et al., 2021), there is an urgent need for residents and policymakers in South and Southeast Asia to know accurately how the onset of B–S monsoon will change in the future.

The B–S monsoon onset is projected to be delayed in the future based on multi-model mean (MMM) results from the third and fifth phases of the Coupled Model Intercomparison Project (CMIP3 and CMIP5) ensemble (Dong et al., 2016; Kitoh & Uchiyama, 2006); however, the delay shows a large spread across models (Moon &

Ha, 2017; Zhang et al., 2012). Some models in the CMIP6 ensemble project a delay in the onset of more than 15 days, while others show an advance of more than 5 days (Wang et al., 2024). This large intermodel uncertainty undermines the credibility of the estimates, and therefore identifying the uncertainty sources and constraining the projections is urgent.

An "emergent relationship" refers to an empirical intermodel relationship between simulation biases in the present-day climate and projected changes in the future climate, which is also supported by physical mechanisms (Bowman et al., 2018; Hall & Qu, 2006). If this relationship can be found, uncertainties in climate change projections can be reduced by calibrating historical simulations against observations (Chen et al., 2020; Chen et al., 2022; Dai et al., 2024; Deangelis et al., 2015; Donat et al., 2018; Dong et al., 2021). This technique, called emergent constraint (EC), has been used to constrain future changes in summer monsoon precipitation (Li et al., 2016, 2017), but not for summer monsoon onset. In this study, we will use the EC technique to rectify future projections of the B–S monsoon onset based on CMIP6 models under the highest emission scenario.

2. Data and Methods

The historical simulations and future projections under the Shared Socioeconomic Pathway 5–8.5 (SSP585) from 25 CMIP6 (Eyring et al., 2016; O'Neill et al., 2016) models (Table S1 in Supporting Information S1) are utilized, based on the availability of daily precipitation in their outputs, and only one realization (i.e., r1i1p1f1) is employed for each model. The future change of a given variable, denoted by "Δ", is defined as the difference between SSP585 (2049–2099) and Historical (1960–2010) periods. Using a climatology with a half-century long period is to remove the effect of internal variability as much as possible. The validation observational data includes six commonly used monthly SST datasets during the period of 1960–2010, including HadISST (Rayner et al., 2003), ERSSTv3 (Smith et al., 2008), ERSSTv5 (Huang et al., 2017), ICOADS (Freeman et al., 2017), COBE-SST (Ishii et al., 2005), and COBE-SST2 (Hirahara et al., 2014). All data are regridded onto a 2.5° grid using bilinear interpolation.

Given the existence of systematic biases in model simulations with respect to observations, it is impractical to directly apply monsoon onset indicators derived from observational data to model results. Therefore, a proxy index is needed to indicate the changes in B–S monsoon onset in model simulations. Here, the May-averaged value of daily time series of accumulated precipitation (AcP) since April 1 (Dunning et al., 2016; Sperber & Annamalai, 2014) is used as the proxy index. Compared to the daily time series of precipitation, the time series of AcP can better reflect the increase of precipitation due to monsoon onset (Figure S1 in Supporting Information S1). The monsoon onset calculated by the AcP starting from different dates (i.e., April 1, 5, 10) have been examined, and the results are insensitive to the start date for accumulating precipitation (Figures not shown). Additionally, the observational monsoon onset variation obtained by AcP and other widely used monsoon onset indexes (Text S1 in Supporting Information S1) defined by previous work (e.g., Kajikawa & Wang, 2012; Xing et al., 2016) have been compared (Figure S2 in Supporting Information S1); their good consistence justifies the good performance of the AcP index in capturing the monsoon onset variations. Therefore, the subsequent analysis uses the future change of the AcP index (i.e., ΔAcP) to represent the temporal change of the monsoon onset date in the future. The underlying physical concept is straightforward: an increase (decrease) in AcP of May is indicative of an earlier (delayed) monsoon onset. Note that we have reversed its sign so that a positive (negative) value of ΔAcP indicates that the monsoon onset will become later (earlier).

The hierarchical emergent constraint framework used to constrain the monsoon onset projections is introduced in Text S2 Supporting Information S1.

3. Results

3.1. Model Spread in Future Changes of Monsoon Onset

Figure 1a shows the key BoB and SCS domains for defining the monsoon onset in this study, where the earliest break out of the Asian summer monsoon is observed (B. Wang & LinHo, 2002). According to the monsoon onset changes obtained from individual models (Figure 1b), we find that although the MMM result (blue dot) shows a delayed monsoon onset in both regions, the projections are highly uncertain between models. Specifically, MIROC6 projects the most advanced monsoon onset (green dot), while ACCESS-CM2 projects the most delayed onset (red dot). To illustrate the intermodel difference, the two extreme model results are compared (Figures 1c

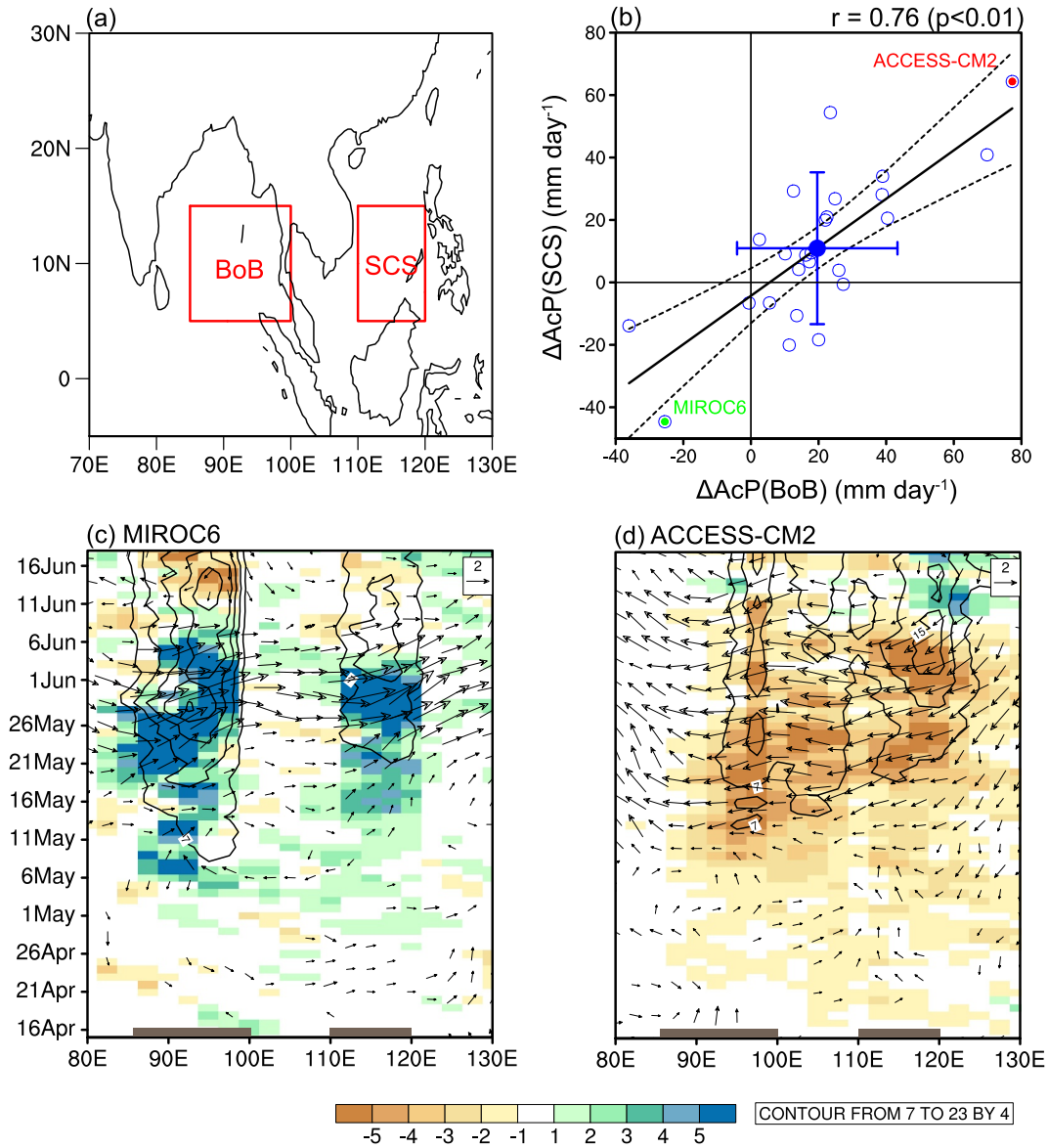

Figure 1. (a) Map showing the BoB (5°–15°N, 85°–100°E) and SCS (5°–15°N, 110°–120°E) with red boxes. (b) Future monsoon onset changes estimated by ΔAcP (mm day^{-1}) for individual models (circles). The green, red, and blue dots denote the results corresponding to MIROC6, ACCESS-CM2, and multi-model average, respectively. The blue horizontal (vertical) line denotes one standard deviation of ΔAcP(BoB) (ΔAcP(SCS)). The black best-fit line is obtained by the least-squares method, and dashed curves represent the 95% confidence range of the linear fit. (c)–(d) Daily climatology of precipitation (contours with an interval of 4 mm day^{-1}) averaged over 5°–15°N in the present period for (c) MIROC6 and (d) ACCESS-CM2, and the future changes in precipitation (shading; mm day^{-1}) and 850 hPa wind (vectors; m s^{-1}). The gray bold lines at the bottom mark the BoB and SCS regions.

and 1d). For both models, a rainbelt is established in May over the BoB and the SCS, signaling the summer monsoon onset. A closer look reveals that the monsoon rainbelt occurs earlier over the BoB than over the SCS, which agrees with observations (Chen & Wang, 2023; Liu et al., 2002; Wang & LinHo, 2002). In the future, MIROC6 (ACCESS-CM2) projects a significant 850 hPa westerly (easterly) anomaly and positive (negative) precipitation anomaly in May over both the BoB and SCS regions. As earlier (delayed) establishment of low-level westerly wind corresponds to earlier (delayed) onset of B–S monsoon, the circulation and precipitation changes are in accordance with the monsoon onset changes indicated by ΔAcP, which further demonstrates the reliability of the AcP-based proxy index.

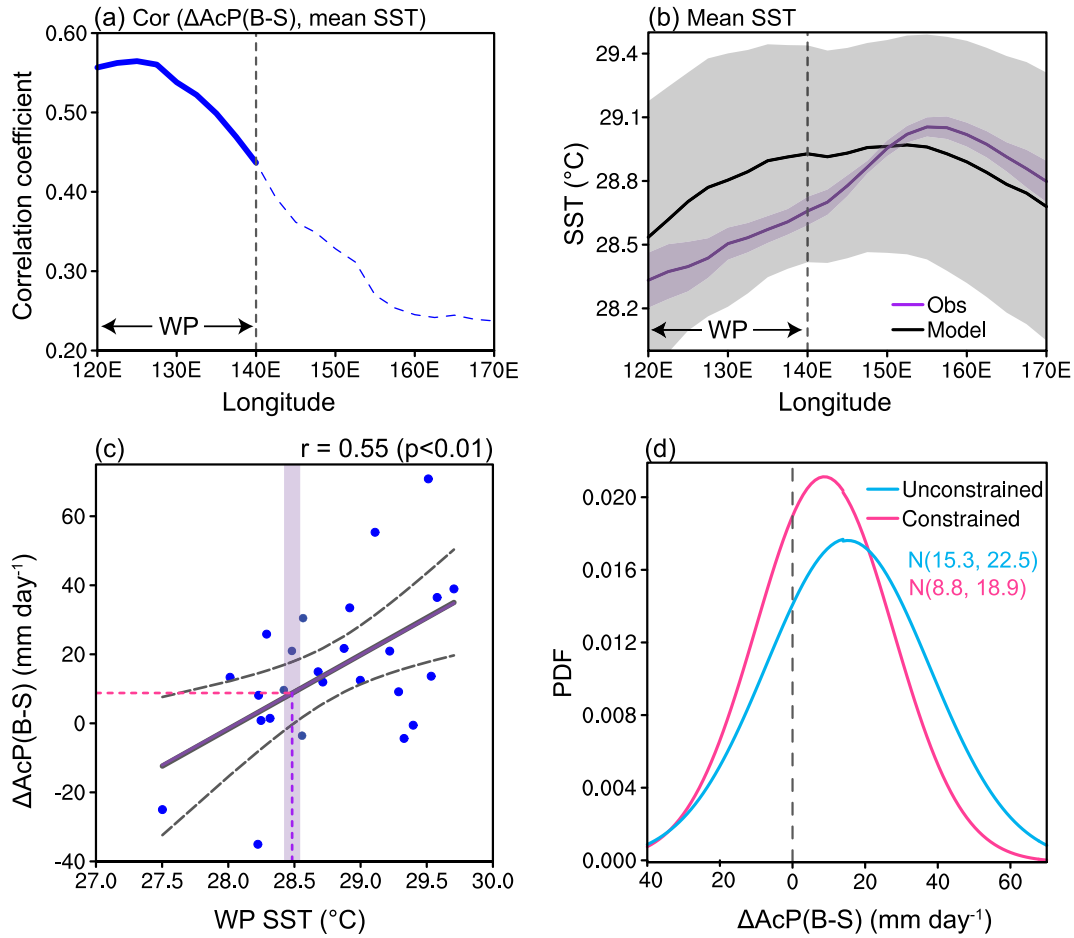

Figure 2. (a) Correlation coefficients between ΔAcP(B–S) and present-day mean SST in spring (February–March average) along the equator (10°S–10°N average), with those above the 95% significance level in bold solid line. (b) Present-day mean spring SST (°C) along the equator corresponding to the mean of multi-models (black solid curve) and the mean of multiple observations (purple curve). The shading denotes one standard deviation of the CMIP6 models and observations, respectively. (c) Scatter plot of ΔAcP(B–S) (mm day^{-1}) versus present-day mean spring SST averaged over the WP (120°–140°E, 10°S–10°N). The gray best-fit line is obtained by the least-squares method, and the gray dashed curves represent the 95% confidence range of the linear fit. The purple best-fit line is obtained by correcting the gray best-fit line based on observations. The vertical purple line denotes the observational WP spring SST averaged over six datasets and the shading denotes one standard deviation limits. The horizontal violet-red line marks the constrained projection result. (d) Probability density function (PDF) of ΔAcP(B–S) generated under a Gaussian assumption for the unconstrained (deepskyblue) and constrained (violet-red) results. The values in parentheses are the mean and one standard deviation of the Gaussian distribution.

Existing studies have shown that the variations in the onset of monsoon over the BoB and SCS regions have the same pace on decadal time scale (e.g., Hu et al., 2022; Xiang & Wang, 2013) as well as in future projections obtained by multi-model mean result (Wang et al., 2024), and demonstrated that the onset changes over these two regions are controlled by common factors. Here, the high intermodel correlation of the future monsoon onset changes between the two regions ($r = 0.76$, $p < 0.01$; Figure 1b) is consistent with previous studies, and is indicative of the common source of the intermodel spread in future monsoon onset changes over the two regions. Therefore, the subsequent analysis combines the AcP index of the two regions (i.e., ΔAcP(B–S)), which is calculated by averaging the values of ΔAcP(BoB) and ΔAcP(SCS). ΔAcP(B–S) agrees with the monsoon onset change over each subregion very well (Figure S3 in Supporting Information S1).

3.2. Applying an Emergent Constraint to Bay of Bengal/South China Sea Monsoon Onset Projections

Figure 2a shows that the B–S monsoon onset future changes are significantly correlated with the mean-state SST over the tropical western Pacific (WP; 10°S–10°N, 120°E−140°E) during February–March in present-day simulations. This means that models simulating a warmer spring SST over the WP in the present-day tend to project a more delayed onset of the B–S monsoon. Despite some observational uncertainty, the simulated WP SST is warmer than the observations, indicating an evident warm bias over the WP for CMIP6 models (Figure 2b). This suggests that future projections of monsoon onset may be constrained by removing the bias in WP SST. The WP-averaged spring SST in the present-day climate is highly correlated with ΔAcP(B–S), with an intermodal correlation of 0.55, significant at the 99% confidence level according to the Student's *t*-test (Figure 2c). Hence, the spread of present-day WP SST in the CMIP6 models can explain around 30% of the intermodel spread in B–S monsoon onset changes. Next, the B–S monsoon onset index, that is, ΔAcP(B–S), is rectified to the observed WP-average SST index using the emergent constraint technique (Text S2 in Supporting Information S1). After constraint, the ΔAcP(B–S) has changed from the raw 15.3 ± 22.5 mm day^{-1} to 8.8 ± 18.9 mm day^{-1} (Figure 2d). The constrained result shows a narrower intermodel spread compared to the raw projection, with 30% reduction in the intermodel variance, and the projected delay in the monsoon onset from the MMM becomes less than before constraint.

To assess the reliability of the constrained projections, we validate the results based on a perfect model hypothesis (Chen et al., 2023; Hu et al., 2024). Each model is sequentially treated as a pseudo-observation, and the remaining models are used to calculate the projected monsoon onset index with and without EC approaches (Text S3 in Supporting Information S1). Compared to the unconstrained projection, the constrained projection is closer to the pseudo-observation for most models (Figure S4 in Supporting Information S1), indicating the effectiveness of the emergent constraint results.

It is important to note that there are other approaches to ensure the robustness of the emergent constraint results, such as out-of-sample testing (Hall et al., 2019). If a given emergent relationship can be obtained from a model ensemble independent of the one in which it was originally proposed, then this emergent relationship can be considered robust. Therefore, it is of interest to conduct a parallel analysis to investigate whether the current emergent relationship based on CMIP6 models can also take place in the other generations of CMIP models.

Subsequently, we use the constrained ΔAcP(B–S) to rectify the projected monsoon onset over the BoB and SCS, respectively, based on their significant linearly correlated relationship in observations (Figure S5 in Supporting Information S1). The constrained projections show a delay of the monsoon onset over the BoB (SCS) by around 2 (3) days, while the unconstrained projections show a delay of about 4 (6) days. This suggests that the previously projected delay in the monsoon onset in the future warmer climate has been overestimated.

3.3. Physical Processes Underpinning the Emergent Relationship

How does the present-day WP spring SST affect the spread in projected changes in the onset of the B–S monsoon? By analysis of the MMM results from CMIP6, Wang et al. (2024) revealed that the delayed B–S monsoon onset in the future is primarily attributed to the enhanced upper-level westerly wind over South Asia prior to monsoon onset, which is caused by stronger upper-tropospheric warming in the tropics relative to the mid-latitudes. A warmer upper troposphere can enhance the westerly vertical shear, which in turn impedes the northward migration of intraseasonal oscillation away from the equator. Since pre-monsoon intraseasonal oscillation is a critical trigger for the onset of B–S monsoon (Li et al., 2018; Wang et al., 2018), delayed establishment of the pre-monsoon intraseasonal oscillation could postpone the subsequent monsoon onset.

The intermodel variation in projected changes in the onset of the B–S monsoon can also be explained by the spread in projected changes in the upper-tropospheric tropical warming and its associated zonal wind anomaly over South Asia (Figure 3a). This indicates that models projecting a more delayed onset of the B–S monsoon are associated with a stronger upper-tropospheric warming in the deep tropics, which in turn leads to a stronger upper-level westerly anomaly near South Asia according to the thermal wind relationship. Furthermore, the atmospheric warming in the deep tropics is likely contributed by positive SST anomalies over both the equatorial Pacific and the southwestern Indian Ocean (Figure 3b). The positive SST anomaly over the equatorial Pacific could induce warming in the mid-to-upper troposphere through a moist adiabatic adjustment process (Held & Soden, 2006; Su et al., 2003), which can spread horizontally throughout the tropics due to equatorial wave adjustments (Neelin &

10.1029/2024GL110994

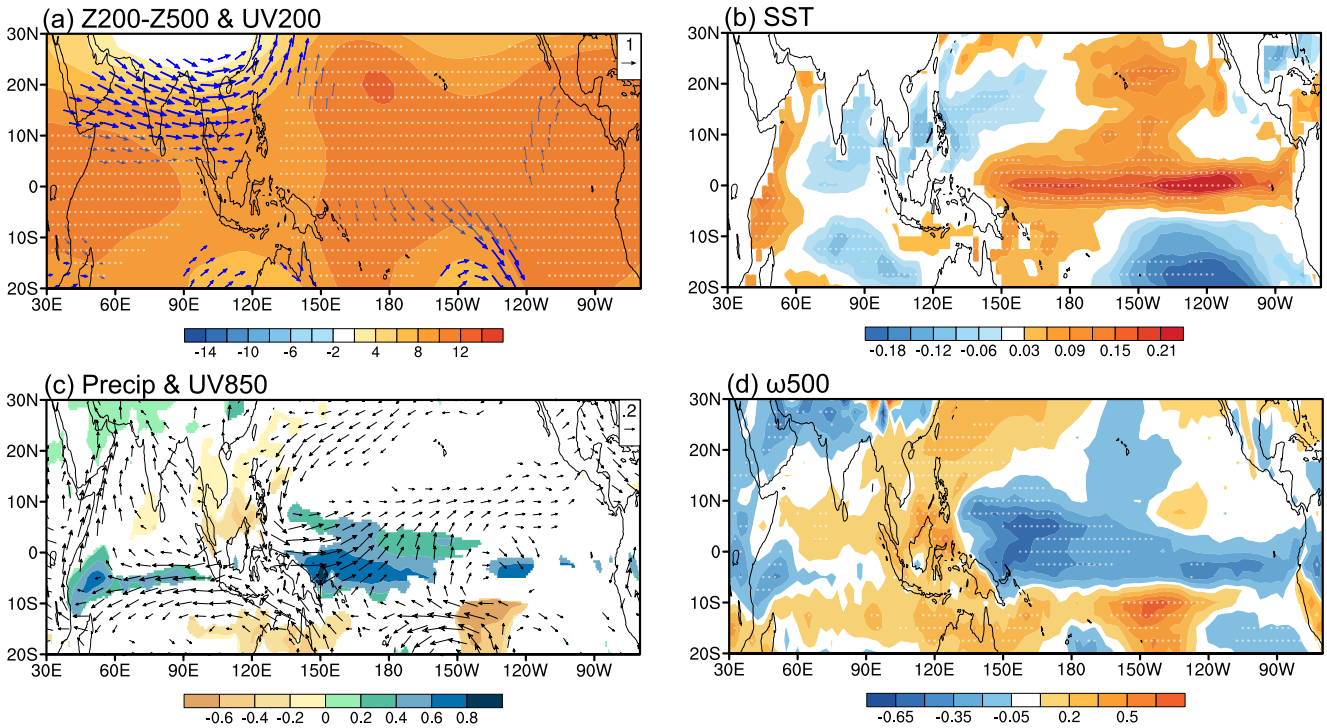

Figure 3. Projected changes in (a) 500–200 hPa thickness (shading; m) and 200 hPa wind (vectors; m s^{-1}), (b) SST (°C), (c) precipitation (shading exceeding the 90% significance level; mm day^{-1}) and 850 hPa wind (vectors; m s^{-1}), (d) 500 hPa vertical velocity (hPa s^{-1}) during February–March regressed onto the normalized ΔAcP (B–S) among models. The regions in (a, b, d) exceeding the 90% significance level are marked by white dots.

Su, 2005; Xie et al., 2010). Meanwhile, the positive SST anomaly over the southwestern Indian Ocean facilitates nearby convection (Figure 3c), which can induce atmospheric warming by the release of condensational latent heat.

To further corroborate the effect of the projected changes in SST on the atmosphere, we regress the atmospheric thickness and upper-level wind against the SST changes over the equatorial Pacific and the southwestern Indian Ocean, respectively (Figure S6 in Supporting Information S1). The projected changes in atmospheric circulation associated with the changes in SST over the two key regions are consistent with those shown in Figure 3a, indicating their significant relationship.

Then, what causes the positive SST anomalies over the equatorial Pacific and southwestern Indian Ocean? We propose that the enhanced precipitation anomaly over the equatorial western-central Pacific (WCP) plays a key role. The WCP convection, on one hand, induces a low-level westerly anomaly over the western Pacific (Figure 3c). This westerly anomaly can drive a downwelling oceanic Kelvin wave as well as an eastward ocean current, which together facilitate warming of the equatorial Pacific through both thermocline and advective processes. On the other hand, the WCP convection weakens the Walker circulation (Figure 3d), which suppresses convection over the Maritime Continent and induces a low-level easterly anomaly along the equatorial Indian Ocean (Figure 3c). The easterly anomaly can drive a westward ocean current that advects warm water from the warm pool region to the western Indian Ocean, favoring warming of the southwestern Indian Ocean.

To elucidate the relationship between the projected changes in WCP precipitation and the present-day WP SST, the top five models that produce the highest WP SST in historical simulations are selected (warm-WP models hereafter); likewise, the five coldest models are selected (cold-WP models). The equatorial SST composite for the warm-WP models peaks near 130°E, but that composite for the cold-WP models peaks near 155°E (Figure 4a). To reveal the strength of atmospheric response to oceanic warming among different models, we further examine the precipitation sensitivity (i.e., $\partial Pr/\partial SST$), which is defined as the linear response of precipitation to SST over the region (10°S–10°N, 120°–170°E) on the interannual time scale (Pathirana et al., 2023). The precipitation sensitivity index peaks near 155°E for the warm-WP models, but near 130°E for the cold-WP models (Figure 4b).

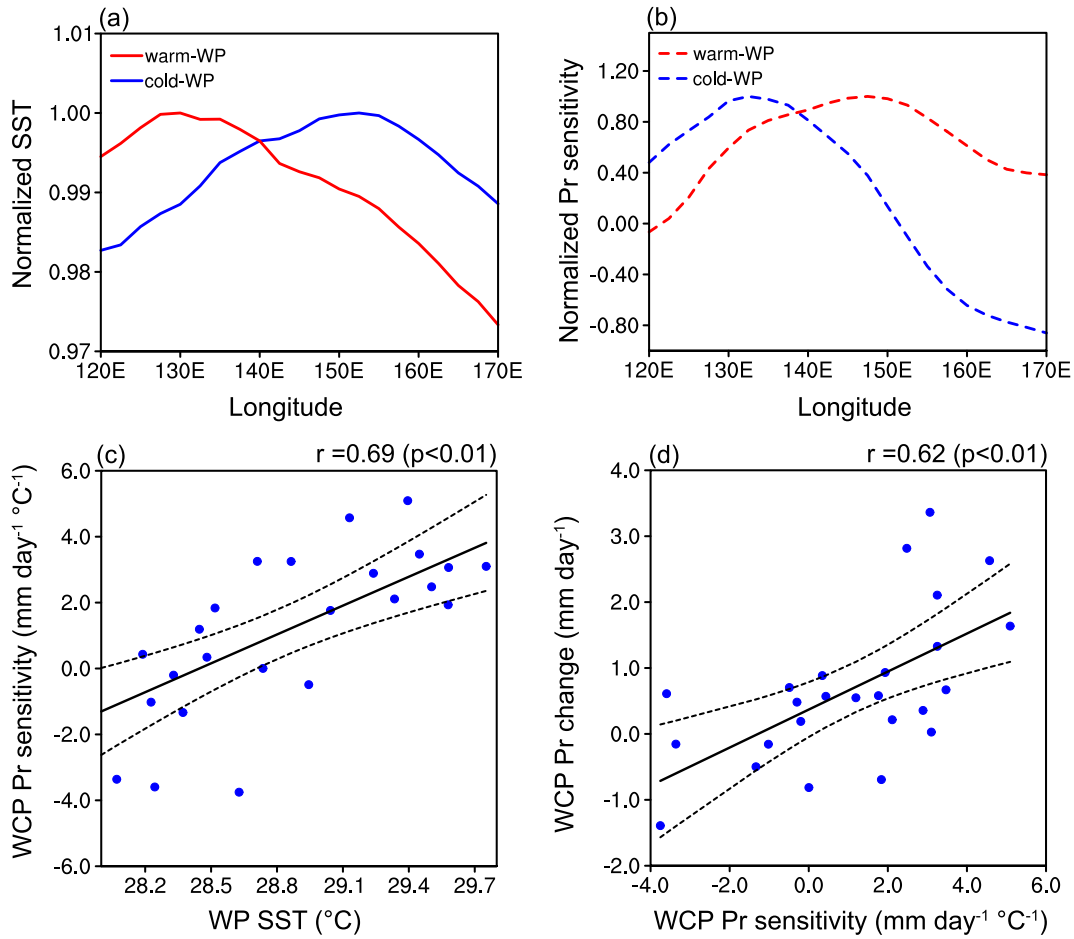

Figure 4. Zonal (10°S–10°N average) distribution of normalized (a) mean SST and (b) precipitation sensitivity during spring (February–March mean) for the warm-WP (red) and cold-WP (blue) groups. Scatter plots of (c) present-day WP (10°S–10°N, 120°–140°E) SST (°C) versus WCP (5°S–5°N, 140°–170°E) precipitation sensitivity (mm day^{-1} °C^{-1}), (d) WCP precipitation sensitivity versus WCP precipitation changes (mm day^{-1}). The solid best-fit line is obtained by the least-squares method, and dashed curves represent the 95% confidence range of the linear fit. The intermodel correlation coefficient (r) and p-value are shown on the top right corner.

The reversed zonal distributions of peaks in SST and precipitation sensitivity indicate that a cooler SST background corresponds to a stronger precipitation response, but a very warm SST background corresponds to a weaker precipitation response (Pathirana et al., 2023; Yun et al., 2021). This intermodel relationship can be further confirmed by the positive correlation coefficient between the WP SST and the WCP precipitation sensitivity ($r = 0.69$, $p < 0.01$; Figure 4c). Given the disparate precipitation sensitivities across models for the WCP, it is reasonable to anticipate that the future precipitation change over this region will vary considerably. The projected change in WCP precipitation is significantly correlated with the present-day precipitation sensitivity ($r = 0.62$, $p < 0.01$; Figure 4d), indicating that models with a larger precipitation sensitivity tend to project a higher increase in precipitation in the future warmer climate.

In summary, models simulating a warmer WP SST in the present show a higher precipitation sensitivity over the WCP, projecting a higher future increase in precipitation over the WCP; the latter facilitates tropical atmospheric warming through inducing positive SST anomalies over the equatorial Pacific and southwestern Indian Ocean, and results in a stronger upper-level westerly anomaly over South Asia, which favors a more delayed onset of the B–S monsoon. It is worth noting that the physical connection between the present-day SST over the WP and the future precipitation change over the WCP, an essential intermediate link to understand the emergent relationship between the present-day WP SST and the projected changes in the onset of the B–S monsoon, could be interpreted differently (Park, Yeh, Min, & Son, 2022; Park, Yeh, Min, & Ham, et al., 2022). Since a strong SST over the WP

indicates a large warm pool area, the models with a warmer WP SST in the present-day simulations tend to simulate a larger reduction in the future zonal SST gradient of the tropical Pacific, weakening the Walker circulation and thereby inducing a larger increase in WCP precipitation. Nevertheless, whichever physical explanation is adopted, it supports the use of the WP SST as an observational constraint for future projections.

4. Conclusions

The onset of the summer monsoon over the Bay of Bengal and the South China Sea typically occurs in early to mid-May, and it is projected to be delayed by the end of 21st century based on multi-model average results of CMIP6 models. However, the extent of the temporal shift of the monsoon onset date in projections exhibits a large spread among models, which undermines the reliability of the multi-model mean result. Here, we find that the present-day mean SST over the tropical western Pacific during boreal spring can contribute to the projection uncertainty in the B–S monsoon onset change, evidenced by their significant intermodel correlation of 0.55. This emergent relationship is attributed to diverse responses of precipitation over the WCP to the WP SST among models. Models with warmer springtime SST over the WP in the present-day climate show higher precipitation sensitivity over the WCP, which leads to more precipitation over the WCP in response to future warming. This, in turn, can result in stronger tropical atmospheric warming, as it can induce positive SST anomalies over the equatorial Pacific and southwestern Indian Ocean through inducing oceanic processes. According to the thermal wind relationship, stronger tropical atmospheric warming results in stronger upper-level westerly anomalies over South Asia, enhancing westerly vertical shear over South Asia and thus favoring a more delayed onset of the B–S monsoon. Compared to unconstrained projections, the constrained projections based on the emergent constraint of WP SST reduce the intermodel uncertainty of the B–S monsoon onset change by 30%, and the projected delay to the onset is almost halved. This suggests that the previously projected delay in the monsoon onset in the future warmer climate has been overestimated, which means that the severity of the originally expected decline in agricultural production and the delayed start of the fishing moratorium were also overestimated, reducing the pressure to adapt to climate change. Furthermore, a more accurate simulation of the WP SST in the present-day climate is crucial for reliable future projections of the monsoon onset.

Data Availability Statement

The CMIP6 data are provided by the Earth System Grid Federation at https://esgf-node.llnl.gov/search/cmip6/. Observational HadISST SST data are available at https://www.metoffice.gov.uk/hadobs/hadisst/. ERSSTv3, ERSSTv5, ICOADS, COBE-SST, and COBE-SST2 are available at https://www.esrl.noaa.gov/psd/data/gridded/tables/sst.html.

Acknowledgments
The work is supported by the National Key Research and Development Program of China (Grant 2020YFA0608901). AT was funded by the MiLCMOP project (Natural Environment Research Council grant number NE/X000176/1). We acknowledge the High Performance Computing Center of Nanjing University of Information Science & Technology for their support of this work.

References

Arias, P.A., Bellouin, N., Coppola, E., Jones, R.G., Krinner, G., Marotzke, J. V., et al. (2021). Technical Summary. In V. Masson-Delmotte, P. Zhai, A. Pirani, S.L. Connors, C. Péan, S. Berger, et al. (Eds.), *Climate change 2021: The physical science basis. Contribution of Working Group I to the Sixth Assessment Report of the Intergovernmental Panel on Climate Change* (pp. 33–144). Cambridge University Press. https://doi.org/10.1017/9781009157896.002

Bombardi, R. J., Kinter, J. L., & Frauenfeld, O. W. (2019). A global gridded dataset of the characteristics of the rainy and dry seasons. *Bulletin of the American Meteorological Society*, *100*(7), 1315–1328. https://doi.org/10.1175/BAMS-D-18-0177.1

Bowman, K. W., Cressie, N., Qu, X., & Hall, A. (2018). A hierarchical statistical framework for emergent constraints: Application to snow-albedo feedback. *Geophysical Research Letters*, *45*(3), 13050–13059. https://doi.org/10.1029/2018GL080082

Chen, H., & Wang, L. (2023). Mechanism of the late summer monsoon onset in Bay of Bengal and South China Sea during 2021: Impacts of intraseasonal oscillation and local thermal contrast. *Dynamics of Atmospheres and Oceans*, *101*, 101348. https://doi.org/10.1016/j.dynatmoce.2022.101348

Chen, X., Zhou, T., Wu, P., Guo, Z., & Wang, M. (2020). Emergent constraints on future projections of the western North Pacific subtropical high. *Nature Communications*, *11*(1), 2802. https://doi.org/10.1038/s41467-020-16631-9

Chen, Z., Zhou, T., Chen, X., Zhang, W., Zhang, L., Wu, M., & Zou, L. (2022). Observationally constrained projection of Afro–Asian monsoon precipitation. *Nature Communications*, *13*(1), 2552. https://doi.org/10.1038/s41467-022-30106-z

Chen, Z., Zhou, T., Chen, X., Zhang, W., Zuo, M., Man, W., & Qian, Y. (2023). Emergent constrained projections of mean and extreme warming in China. *Geophysical Research Letters*, *50*(20), e2022GL102124. https://doi.org/10.1029/2022GL102124

Dai, P., Nie, J., Yu, Y., & Wu, R. (2024). Constraints on regional projections of mean and extreme precipitation under warming. *Proceedings of the National Academy of Sciences*, *121*(11), e2312400121. https://doi.org/10.1073/pnas.2312400121

DeAngelis, A. M., Qu, X., Zelinka, M. D., & Hall, A. (2015). An observational radiative constraint on hydrologic cycle intensification. *Nature*, *528*(7581), 249–253. https://doi.org/10.1038/nature15770

Donat, M. G., Pitman, A. J., & Angélil, O. (2018). Understanding and reducing future uncertainty in midlatitude daily heat extremes via land surface feedback constraints. *Geophysical Research Letters*, *45*(19), 10–627. https://doi.org/10.1029/2018GL079128

Dong, G., Zhang, H., Moise, A., Hanson, L., Liang, P., & Ye, H. (2016). CMIP5 model-simulated onset, duration and intensity of the Asian summer monsoon in current and future climate. *Climate Dynamics*, *46*(1–2), 355–382. https://doi.org/10.1007/s00382-015-2588-z

Dong, L., Leung, L. R., Lu, J., & Song, F. (2021). Double-ITCZ as an emergent constraint for future precipitation over Mediterranean climate regions in the North Hemisphere. *Geophysical Research Letters*, *48*(3), e2020GL091569. https://doi.org/10.1029/2020GL091569

Dunning, C. M., Black, E. C., & Allan, R. P. (2016). The onset and cessation of seasonal rainfall over Africa. *Journal of Geophysical Research: Atmospheres*, *121*(19), 11–405. https://doi.org/10.1002/2016JD025428

Eyring, V., Bony, S., Meehl, G. A., Senior, C. A., Stevens, B., Stouffer, R. J., & Taylor, K. E. (2016). Overview of the coupled model intercomparison project phase 6 (CMIP6) experimental design and organization. *Geoscientific Model Development*, *9*(5), 1937–1958. https://doi.org/10.5194/gmd-9-1937-2016

Freeman, E., Woodruff, S. D., Worley, S. J., Lubker, S. J., Kent, E. C., Angel, W. E., et al. (2017). ICOADS release 3.0: A major update to the historical marine climate record. *International Journal of Climatology*, *37*(5), 2211–2237. https://doi.org/10.1002/joc.4775

Hall, A., Cox, P., Huntingford, C., & Klein, S. (2019). Progressing emergent constraints on future climate change. *Nature Climate Change*, *9*(4), 269–278. https://doi.org/10.1038/s41558-019-0436-6

Hall, A., & Qu, X. (2006). Using the current seasonal cycle to constrain snow albedo feedback in future climate change. *Geophysical Research Letters*, *33*(3). https://doi.org/10.1029/2005GL025127

Held, I. M., & Soden, B. J. (2006). Robust responses of the hydrological cycle to global warming. *Journal of Climate*, *19*(21), 5686–5699. https://doi.org/10.1175/JCLI3990.1

Hirahara, S., Ishii, M., & Fukuda, Y. (2014). Centennial-scale sea surface temperature analysis and its uncertainty. *Journal of Climate*, *27*(1), 57–75. https://doi.org/10.1175/JCLI-D-12-00837.1

Hu, P., Chen, W., Chen, S., Liu, Y., Wang, L., & Huang, R. (2022). The leading mode and factors for coherent variations among the sub-systems of tropical Asian summer monsoon onset. *Journal of Climate*, *35*(5), 1597–1612. https://doi.org/10.1175/JCLI-D-21-0101.1

Hu, S., Wang, L., Chen, X., Zhou, T., & Hsu, P. C. (2024). Emergent constraints on future projections of Tibetan Plateau warming in winter. *Geophysical Research Letters*, *51*(9), e2024GL108728. https://doi.org/10.1029/2024GL108728

Huang, B., Thorne, P. W., Banzon, V. F., Boyer, T., Chepurin, G., Lawrimore, J. H., et al. (2017). Extended reconstructed sea surface temperature, version 5 (ERSSTv5): Upgrades, validations, and intercomparisons. *Journal of Climate*, *30*(20), 8179–8205. https://doi.org/10.1175/JCLI-D-16-0836.1

Ishii, M., Shouji, A., Sugimoto, S., & Matsumoto, T. (2005). Objective analyses of sea-surface temperature and marine meteorological variables for the 20th century using ICOADS and the Kobe collection. *International Journal of Climatology*, *25*(7), 865–879. https://doi.org/10.1002/joc.1169

Islam, M. M., Begum, A., Rahman, S. M. A., & Ullah, H. (2021). Seasonal fishery closure in the northern bay of Bengal causes immediate but contrasting ecological and socioeconomic impacts. *Frontiers in Marine Science*, *8*, 704056.

Jiang, X., Wang, Z., & Li, Z. (2018). Signature of the South China Sea summer monsoon onset on spring-to-summer transition of rainfall in the middle and lower reaches of the Yangtze River basin. *Climate Dynamics*, *51*(9–10), 3785–3796. https://doi.org/10.1007/s00382-018-4110-x

Kajikawa, Y., & Wang, B. (2012). Interdecadal change of the South China Sea summer monsoon onset. *Journal of Climate*, *25*(9), 3207–3218. https://doi.org/10.1175/JCLI-D-11-00207.1

Kitoh, A., & Uchiyama, T. (2006). Changes in onset and withdrawal of the East Asian summer rainy season by multi-model global warming experiments. *Journal of the Meteorological Society of Japan*, *84*(2), 247–258. https://doi.org/10.2151/jmsj.84.247

Li, G., Xie, S.-P., Du, Y., & Luo, Y. (2016). Effects of excessive equatorial cold tongue bias on the projections of tropical Pacific climate change. Part I: The warming pattern in CMIP5 multi-model ensemble. *Climate Dynamics*, *47*(12), 3817–3831. https://doi.org/10.1007/s00382-016-3043-5

Li, G., Xie, S.-P., He, C., & Chen, Z. (2017). Western Pacific emergent constraint lowers projected increase in Indian summer monsoon rainfall. *Nature Climate Change*, *7*(10), 708–712. https://doi.org/10.1038/nclimate3387

Li, K., Liu, Y., Li, Z., Yang, Y., Feng, L., Khokiattiwong, S., et al. (2018). Impacts of ENSO on the Bay of Bengal summer monsoon onset via modulating the intraseasonal oscillation. *Geophysical Research Letters*, *45*(10), 5220–5228. https://doi.org/10.1029/2018GL078109

Liu, Y. M., Chan, J. C. L., Mao, J. Y., & Wu, G. X. (2002). The role of Bay of Bengal convection in the onset of the 1998 South China Sea summer monsoon. *Monthly Weather Review*, *130*(11), 2731–2744. https://doi.org/10.1175/1520-0493(2002)130<2731:trobob>2.0.co;2

Moon, S., & Ha, K.-J. (2017). Temperature and precipitation in the context of the annual cycle over Asia: Model evaluation and future change. *Asia-Pacific Journal of Atmospheric Sciences*, *53*(2), 229–242. https://doi.org/10.1007/s13143-017-0024-5

Neelin, J. D., & Su, H. (2005). Moist teleconnection mechanisms for the tropical South American and Atlantic sector. *Journal of Climate*, *18*(18), 3928–3950. https://doi.org/10.1175/JCLI3517.1

O'Neill, B. C., Tebaldi, C., van Vuuren, D. P., Eyring, V., Friedlingstein, P., Hurtt, G., et al. (2016). The scenario model intercomparison project (ScenarioMIP) for CMIP6. *Geoscientific Model Development*, *9*(9), 3461–3482. https://doi.org/10.5194/gmd-9-3461-2016

Park, I.-H., Yeh, S., Min, S., & Son, S. (2022). Emergent constraints on future expansion of the Indo-Pacific warm pool. *Geophysical Research Letters*, *49*(1), e2021GL097343. https://doi.org/10.1029/2021GL097343

Park, I. H., Yeh, S. W., Min, S. K., Ham, Y. G., & Kirtman, B. P. (2022). Present-day warm pool constrains future tropical precipitation. *Communications Earth and Environment*, *3*(1), 310. https://doi.org/10.1038/s43247-022-00620-5

Pathirana, G., Shin, N. Y., Wu, Y. K., Kwon, M., & Kug, J. S. (2023). Intermodel relation between present-day warm pool intensity and future precipitation changes. *Climate Dynamics*, *62*(1s), 345–355. https://doi.org/10.1007/s00382-023-06918-0

Rayner, N. A., Parker, D. E., Horton, E. B., Folland, C. K., Alexander, L. V., Rowell, D. P., et al. (2003). Global analyses of sea surface temperature, sea ice, and night marine air temperature since the late nineteenth century. *Journal of Geophysical Research*, *108*(D14), 4407. https://doi.org/10.1029/2002JD002670

Smith, T. M., Reynolds, R. W., Peterson, T. C., & Lawrimore, J. (2008). Improvements to NOAA's Historical Merged Land–Ocean Surface Temperature Analysis (1880–2006). *Journal of Climate*, *21*(10), 2283–2296. https://doi.org/10.1175/2007JCLI2100.1

Sperber, K. R., & Annamalai, H. (2014). The use of fractional accumulated precipitation for the evaluation of the annual cycle of monsoons. *Climate Dynamics*, *43*(12), 3219–3244. https://doi.org/10.1007/s00382-014-2099-3

Su, H., Neelin, J. D., & Meyerson, J. E. (2003). Sensitivity of tropical tropospheric temperature to sea surface temperature forcing. *Journal of Climate*, *16*(9), 1283–1301. https://doi.org/10.1175/1520-0442-16.9.1283

Wang, B., & LinHo. (2002). Rainy season of the Asian–Pacific summer monsoon. *Journal of Climate*, *15*(4), 386–398. https://doi.org/10.1175/1520-0442(2002)015<0386:RSOTAP>2.0.CO;2

Wang, H., Liu, F., Wang, B., & Li, T. (2018). Effects of intraseasonal oscillation on South China Sea summer monsoon onset. *Climate Dynamics*, *51*(7–8), 2543–2558. https://doi.org/10.1007/s00382-017-4027-9

Wang, L., & Chen, G. (2018). Relationship between South China Sea summer monsoon onset and landfalling tropical cyclone frequency in China. *International Journal of Climatology*, *38*(7), 3209–3214. https://doi.org/10.1002/joc.5485

Wang, L., Cheng, Y., Chen, X., & Zhou, T. (2024). Projected changes in onset of summer monsoon over the South Asian marginal seas modulated by intraseasonal oscillation. *Journal of Climate*, *37*(3), 821–835. https://doi.org/10.1175/JCLI-D-23-0257.1

Xiang, B., & Wang, B. (2013). Mechanisms for the advanced Asian summer monsoon onset since the mid-to-late 1990s. *Journal of Climate*, *26*(6), 1993–2009. https://doi.org/10.1175/JCLI-D-12-00445.1

Xie, S. P., Deser, C., Vecchi, G. A., Ma, J., Teng, H., & Wittenberg, A. T. (2010). Global warming pattern formation: Sea surface temperature and rainfall. *Journal of Climate*, *23*(4), 966–986. https://doi.org/10.1175/2009JCLI3329.1

Xing, N., Li, J., Jiang, X., & Wang, L. (2016). Local oceanic precursors for the summer monsoon onset over the Bay of Bengal and the underlying processes. *Journal of Climate*, *29*(3), 8455–8470. https://doi.org/10.1175/JCLI-D-15-0825.1

Yun, K. S., Lee, J. Y., Timmermann, A., Stein, K., Stuecker, M. F., Fyfe, J. C., & Chung, E. S. (2021). Increasing ENSO–rainfall variability due to changes in future tropical temperature–rainfall relationship. *Communications Earth and Environment*, *2*(1), 43. https://doi.org/10.1038/s43247-021-00108-8

Zhang, H., Liang, P., Moise, A., & Hanson, L. (2012). Diagnosing potential changes in Asian summer monsoon onset and duration in IPCC AR4 model simulations using moisture and wind indices. *Climate Dynamics*, *39*(9–10), 2465–2486. https://doi.org/10.1007/s00382-012-1289-0

References From the Supporting Information

Adler, R. F., et al. (2003). The version-2 Global Precipitation Climatology Project (GPCP) monthly precipitation analysis (1979–present). *Journal of Hydrometeorology*, *4*(6), 1147–1167. https://doi.org/10.1175/1525-7541(2003)004<1147:TVGPCP>2.0.CO;2

Dee, D. P., Uppala, S. M., Simmons, A. J., Berrisford, P., Poli, P., Kobayashi, S., … & Vitart, F. (2011). The ERA-Interim reanalysis: Configuration and performance of the data assimilation system. *Quarterly Journal of the Royal Meteorological Society*, *137*(656), 553-597. https://doi.org/10.1002/qj.828

Wang, M. M., Begum, A., Rahman, S. M. A., & Ullah, H. (2021). Seasonal fishery closure in the northern Bay of Bengal causes immediate but contrasting ecological and socioeconomic impacts. *Frontiers in Marine Science*, *8*, 704056. https://doi.org/10.3389/fmars.2021.704056